

Strength and microstructural analysis of concrete incorporating ash from sunflower seed shells combustion

Netinger Grubeša, Ivanka; Radeka, Miroslava; Malešev, Mirjana; Radonjanin, Vlastimir; Gojević, Anita; Siddique, Rafat

Source / Izvornik: **Structural Concrete, 2019, 20, 396 - 404**

Journal article, Published version

Rad u časopisu, Objavljena verzija rada (izdavačev PDF)

<https://doi.org/10.1002/suco.201800036>

Permanent link / Trajna poveznica: <https://um.nsk.hr/um:nbn:hr:133:562934>

Rights / Prava: [Attribution 4.0 International](#)/[Imenovanje 4.0 međunarodna](#)

Download date / Datum preuzimanja: **2025-03-06**



GRAĐEVINSKI I ARHITEKTONSKI FAKULTET OSIJEK
Faculty of Civil Engineering and Architecture Osijek


Repository / Repozitorij:

[Repository GrAFOS - Repository of Faculty of Civil Engineering and Architecture Osijek](#)



TECHNICAL PAPER

Strength and microstructural analysis of concrete incorporating ash from sunflower seed shells combustion

Ivanka N. Grubeša¹  | Miroslava Radeka² | Mirjana Malešev² | Vlastimir Radonjanin² | Anita Gojević³ | Rafat Siddique⁴

¹Faculty of Civil Engineering Osijek, Josip Juraj Strossmayer University of Osijek, Osijek, Croatia

²Department of Civil Engineering and Geodesy, Faculty of Technical Sciences, University in Novi Sad, Novi Sad, Serbia

³Josip Juraj Strossmayer University of Osijek, Osijek, Croatia

⁴Department of Civil Engineering, Thapar University, Patiala, Punjab, India

Correspondence

Ivanka N. Grubeša, Faculty of Civil Engineering Osijek, Josip J. Strossmayer University of Osijek, Drinska 16a, 31000 Osijek, Croatia
Email: nivanka@gfos.hr

The aim of the study involves determining the added value of shells of sunflower seeds ash (SSA) as a mineral admixture in concrete and the effects/mechanisms through which it affects the concrete microstructure. The chemical effect of this type of ash was estimated by examining its chemical composition, pozzolanic activity index, and *SEM* investigation while its physical effect was observed at the level of concrete with ash incorporated. Four concrete mixtures with different shares of cement replacement by ash were prepared (0, 5, 7.5, and 10%). The water to binder ratio was 0.5, and binder content 400 kg/m³ in all mixtures. The properties of fresh and hardened concrete with ash incorporated were compared with the corresponding properties of the reference concrete. The results indicate that SSA achieved all the known possible effects of mineral admixtures; filler effect, heterogenous nucleation effect, dilution effect, and a certain degree of chemical effect. However, replacing more than 5% of cement mass with SSA will adversely affect mechanical properties of concrete.

KEYWORDS

ash from sunflower seed shells combustion, concrete, mechanical properties, mineral admixture effects, *SEM* analysis

1 | INTRODUCTION

Directive 2009/28/EC on the promotion of the use of energy from renewable sources¹ sets 20% energy from renewable sources for the EU by 2020 as a mandatory target. Based on the directive, the renewable energies correspond to wind energy, solar energy, aerothermal energy, geothermal energy, hydrothermal and ocean energy, hydropower, land-fill gas, sewage treatment plant gas, biogases, and biomass. Biomass refers to any organic material that is derived from plants or animals² that are currently living or lived in the recent past. Biomass is derived from botanical (plant species) or biological (animal waste or carcass) sources or from a combination of the same. Common sources of biomass are as follows³:

- Agricultural: food grain, bagasse (crushed sugarcane), corn stalks, straw, seed hulls, nutshells, and manure from cattle, poultry, and hogs.
- Forest: trees, wood waste, wood or bark, sawdust, timber slash, and mill scrap.
- Municipal: sewage sludge, refuse-derived fuel, food waste, waste paper, and yard clippings.
- Energy crops: poplars, willows, switchgrass, alfalfa, prairie bluestem, corn, soybean, canola, and other plant oils.
- Biological: animal waste, aquatic species, and biological waste.

When biomass is used as a fuel in the industry, the inorganic solid residue left after biomass is completely burned, and is termed as biomass ash. Numerous researchers attempted to determine the possible use of biomass ashes in the field of civil engineering. In road applications, most

Discussion on this paper must be submitted within two months of the print publication. The discussion will then be published in print, along with the authors' closure, if any, approximately nine months after the print publication.

studies focused on the use of biomass ash in soil stabilization^{4–6} owing to its cementing and pozzolanic properties, and promising results were obtained. In addition, various types of biomass ashes (including woodchips, shells, rice husk, wood, refuse-derived fuel, straw, barks, and sludge ashes) were examined as aggregate fillers for bituminous mixtures in Ref. 7 and it is concluded that most ashes can be considered as potential replacements for natural fillers. According to Cuenca et al.⁸ when biomass ashes are used as a filler in self-compacting concrete, they maintain the compressive strength at the same level as that of reference concrete or can even increase its value. However, the most widely investigated topic in scientific studies corresponds to the possibility of applying this type of ash as a partial^{9–15} or complete substitute for cement.^{16–18} Cement replacement with 10, 20, and 30% of various types of ashes was examined by Shrivastava and Jain¹⁵ and the results indicate that rice husk ash, sugarcane bagasse ash, and wheat straw ash, in which a maximum of 10% cement is replaced, maintain the compressive strength of concrete at the same level as that of reference concrete. The durability properties involving corn stalk, wheat straw, and sunflower stalk ashes in amounts corresponding to 2 and 5% relative to the cement mass were investigated in Ref. 9 and it is concluded that all the ashes improved the resistance of concrete to abrasion and freeze–thaw cycles. Improvement in the durability of composites containing wheat straw in terms of resistance to magnesium sulfate and sodium sulfate attack as methods for freeze–thaw resistance estimation is confirmed in Ref. 11. When wheat straw ash is combined with rice husk ash and used to substitute cement for a total of 15%, the composites containing ashes exhibited higher compressive and flexural strengths than control composite. This is explained in terms of a synergy that exists between these ashes because of the optimization of the pozzolanic reaction and filler effect.¹² Although no biomass species were specified, it was observed in Ref. 14 that biomass ashes increase the setting time and reduce the heat of hydration. The increase in setting time is confirmed in (Aliyu). In Ref. 13, the authors suggest that these types of ashes may exhibit high alkali content. However, the characteristics of ashes are influenced by biomass characteristics, combustion technology, and the location where the ashes are collected.¹⁹ This implies that each ash should be individually investigated in a specific application area.

The addition of admixtures mainly affects concrete in two ways, specifically, chemically, or physically, through the heterogenous nucleation, filler, and dilution effects.^{20–29} If the admixture is chemically active, new reaction processes during hydration are introduced or existing reactions are modified. Even if an admixture is inert, the chemical effect is involved in a few hydration reactions.^{22,28} In case of the heterogenous nucleation effect, the added particles enhance the hydration reaction by acting as nucleation sites and become an integrated part of the cement paste. The addition

of filler also dilutes the cement particle system, influences the average distance between cement particles, and influences the water content available for cement hydration. Finally, the filler effect causes the filling of small pores between cement particles by finer powder particles based on the particle size distribution of the cement and filler. All these effects influence the properties of the cement paste, and thereby those of concrete.

Sunflower seed shells are used as a substitute for commonly used fuel in a Croatian oil factory Čepin, cca 7 t of ash per month, and thus, 84 t of ash per year are generated. It is fly ash given its nature, and its only application to date is as a fertilizer for soil enrichment in agriculture.³⁰ Hence, the present study examines the use of this fly ash as a mineral admixture in concrete to determine added value for the ash that also simultaneously lowers the final price of concrete. The present study explores the possibility of applying fly ash generated by the combustion of shells of sunflower seeds in a Croatian oil factory as a partial replacement for cement in concrete. This is part of a wider study that investigates the possible application of certain types of biomass ash in civil engineering structures.

2 | EXPERIMENTAL PROGRAM

2.1 | Material characterization

2.1.1 | Aggregate properties

All concrete mixtures examined in this study were prepared with dolomite aggregate (fractions corresponding to 0–4, 4–8, and 8–16 mm) in which the particle size distribution that was determined according to Ref. 31 is given in Figure 1.

The density of crushed dolomite aggregate was 2.75 kg/dm³ and was tested according to Ref. 32. Aggregate fractions that were used for preparing concrete were first saturated and then surface-dried. This was achieved in an artificial manner by dipping aggregates into a water tank for 24 hr, removing the same, and then wiping excess water from their surfaces.

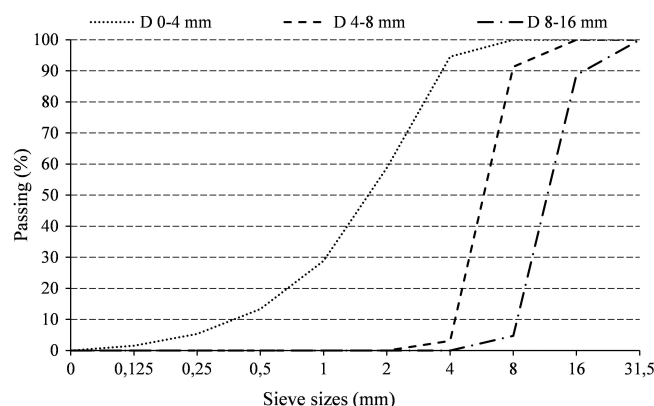


FIGURE 1 Particle size distribution of the aggregate

TABLE 1 Physical and chemical composition of the binders

Constituent	Cement	SSA
Chemical composition (% by mass)		
SiO ₂	20.56	2.03
CaO	59.48	23.33
Al ₂ O ₃	5.25	0.41
Fe ₂ O ₃	1.91	0.73
MgO	2.62	7.73
MnO	0.12	0.12
Na ₂ O	0.23	0.33
K ₂ O	0.60	21.35
SO ₃	3.25	14.51
Cl ⁻	0.002	0.709
S ²⁻	—	0.00
P ₂ O ₅	—	3.48
Insoluble residue (HCl/KOH)	—	1.24
Reactive SiO ₂	—	0.50
Loss on ignition (LOI)	6.17	25.54
Physical properties		
Density (g/cm ³)	3.00	2.15
Blaine surface (m ² /kg)	243.9	337.4
AI at the age of 7 days	—	0.58
AI at the age of 28 days	—	0.51
AI at the age of 90 days	—	0.48

Note. AI: activity index; SSA: sunflower seeds ash.

2.1.2 | Binder properties

The cement used was ordinary Portland cement, CEM I 42.5 R, according to.³³ The chemical and physical properties of the cement and ash from sunflower seeds combustion are listed in Table 1. The chemical analysis of binders was performed based on Ref. 34 by using XRF measurements, while the reactive silica content was determined by wet chemistry based on the same standard. The density and Blaine surface/fineness were measured according to Ref. 35 and the activity index (AI) for sunflower seeds ash (SSA) at ages corresponding to 7, 28, and 90 days were measured according to Ref. 36.

The chemical composition of SSA (Table 1) indicates a very low content of total and reactive SiO₂, and this is characteristic of low-pozzolanic ashes. The content of MgO, K₂O, SO₃, and Cl⁻ ions exceed the proposed values given in Ref. 36. A high value of MgO results in volume instability of the cement paste in which SSA is incorporated (^{37,38}). High values of K₂O and SO₃ can influence the hydration process. The high concentration of K₂O can lead to alkali-silica reactions, and the SO₃ content can lead to the formation of different forms of sulfates while the chloride ion content can contribute to the acceleration of binder hydration. Loss on ignition is commonly attributed to the amount of unburned carbon, and thereby indicates the low efficiency of the combustion process. Its SSA value is considerably high, and this typically reduces its pozzolanic activity.¹⁹ According to Ref. 36, an activity index of 0.8 is required for

materials to be considered as pozzolanic, and the activity indices for SSA are below 0.8.

The particle size distributions of binders (cement and SSA) were determined by the laser diffraction method based on Ref. 39 by using a Malvern Mastersizer 2000 particle size analyzer that can analyze particles between 0.01 and 2,000 μm. The Malvern Mastersizer 2000 records the light pattern scattered from a field of particles at different angles. The recorded intensity at a certain angle is the sum of the intensity of light scattered from the surface of the particles and the intensity of the secondary scattered light because of refraction while passing through the particle, and this is important for particles smaller than 50 μm. The device uses an analytical procedure to determine the particle size distribution that created the patterns. Applied Mie light scattering theory assumes that particles are spheres, and thus, the results obtained for particle diameters specifically correspond to equivalent sphere diameters. The measurements were performed with an automated dry dispersion unit Scirocco 2000. Prior to measurement, several tests were performed to select optimal measuring conditions, namely feed rate and nozzle pressure. The selected feed rate provides adequate obscuration in the range of 3.26–4.15%. The selected nozzle pressure of 2 bar results in good reproducibility of results for all the samples. The sample was analyzed in three replicates. The results were recorded as particle volume percentages and presented in Figure 2, while Table 2 lists the values of d₁₀ (with particle diameters corresponding to 10% of the cumulative undersize distribution by volume), d₅₀ (median particle diameter corresponding to 50% by volume of the particles smaller than this diameter and 50% larger), and d₉₀ (particle diameter corresponding to 90% of the cumulative undersize distribution by volume) for both samples.

The particle size distribution analysis implies that SSA includes finer particles than cement, and thus, the SSA could play the role of a filler. The median diameter of particles, d₅₀, for cement and SSA correspond to 16.192 and

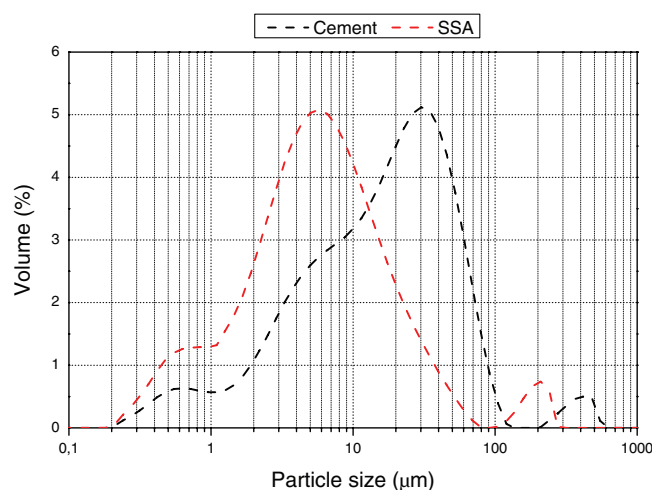
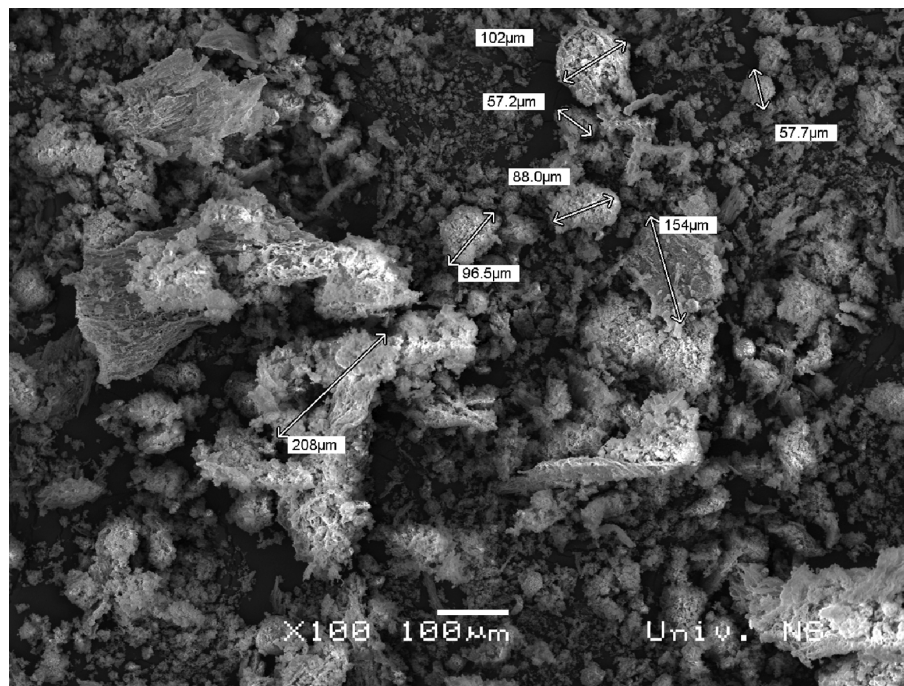


FIGURE 2 Particle size distribution of binders

TABLE 2 Particle size distribution of binders

	d_{10} (μm) (%)	d_{50} (μm) (%)	d_{90} (μm) (%)	Span of distribution
Cement	2.193	16.192	53.378	3.161
SSA	0.941	5.817	25.352	4.196

Note. SSA: sunflower seeds ash.

**FIGURE 3** SEM image of sunflower seeds ash particles ($\times 100$)

5,817 μm , respectively (Table 2). The d_{10} value is subtracted from d_{90} , and this result is divided by d_{50} to calculate the distribution span value. The higher value of the SSA span indicates a broader particle size distribution.

Size frequency distribution (that is presented as a volume percentage) indicates that cement and SSA particles are not uniform in size. A small volume of agglomerated particles with mean diameters of approximately 400 (cement) and 200 μm (SSA) were observed.

The SEM image of SSA is presented in Figure 3. This image shows that SSA contains particles about several micrometers in size and their aggregates with diameters up to 208 μm . Its surface is significantly porous, thereby

indicating that it impacts cement hydration as a mineral admixture. Hence, SSA is not expected to correspond to an inert mineral admixture due to the contents of K_2O , SO_3 , and Cl^- ions. Given the high amount of SO_3 and K_2O , it is highly likely that the formation of different forms of sulfate occurs. At this stage of research, it is concluded that SSA is neither a pozzolanic active nor a completely chemically inert admixture.

2.1.3 | Preparation of concrete mixtures

In this study, four concrete mixtures with different shares of cement replacement by ash from the combustion of shells of sunflower seeds were prepared (0, 5, 7.5, and 10%). Table 3

TABLE 3 Composition of the mixture

Characteristics	M0	M5	M7.5	M10		
Water/binder ratio (w/b)	0.5	0.5	0.5	0.5		
Cement (kg)	400	380	370	360		
Sunflower seeds ash (SSA) (kg)	—	20	30	40		
Water (kg)	200	200	200	200		
Aggregate (kg)	1,764	1,764	1,764	1,764		
Dolomite 0–4 mm (%–kg)	42	741	42	741	42	741
Dolomite 4–8 mm (%–kg)	19	335	19	335	19	335
Dolomite 8–16 mm (%–kg)	39	688	39	688	39	688

TABLE 4 Properties of fresh concrete

Characteristics	M0	M5	M7.5	M10
Density (kg/m ³)	2,433	2,370	2,356	2,343
Air content (%)	2.5	3.0	2.7	3.2
Slump test (mm)	210	30	25	10

lists the proportions of all constituents in the mixtures. With respect to all the mixtures, the water to binder ratio (w/b) was 0.5 with water from the water supply and a binder content of 400 kg/m³. Aggregates, binder, and water were mixed together for 5 min in a pan mixer (DZ 100VS, Diemwerke, Hörbranz, Austria).

2.1.4 | Testing of fresh concrete

The density was tested based on Ref. 40), air content was tested based on Ref. 41, and consistency was tested based on Ref. 42.

2.1.5 | Testing of hardened concrete specimens

Three specimens were prepared to determine each property. Specimens of all concrete mixtures were cast and compacted by using a vibrating table. All specimens were extracted from the molds 24 hr after the casting and placed in a water tank for 27 days at a temperature of $20 \pm 5^\circ\text{C}$ based on Ref. 43. The properties of the hardened concrete specimens were tested as follows:

- The compressive strength was tested on cube specimens with an edge length of 15 cm with a constant rate of loading of 0.5 MPa/s based on Ref. 44 at ages corresponding to 28 and 90 days.
- Flexural strength was tested on prism specimens with dimensions of $10 \times 10 \times 40 \text{ cm}^3$ by loading the same with a constant rate of 0.05 MPa/s based on Ref. 45 at the age of 28 days.
- Static modulus of elasticity was tested on prism specimens with dimensions of $10 \times 10 \times 40 \text{ cm}^3$ based on the procedure described in Ref. 46.
- The morphology of the cross section of samples was assessed by SEM.

TABLE 5 Properties of hardened concrete

Characteristics	M0	M5	M7.5	M10
Compressive strength at 28 days (MPa)	40.80	39.70	37.80	33.70
SD (MPa)	± 1.42	± 1.42	± 0.47	± 1.37
Compressive strength at 90 days (MPa)	47.80	45.20	41.30	39.70
SD (MPa)	± 1.43	± 0.59	± 0.72	± 1.06
Flexural strength (MPa)	5.00	5.60	4.08	5.06
SD (MPa)	± 0.27	± 0.34	± 0.23	± 0.27
Modulus of elasticity (MPa)	25,942	25,157	24,753	22,766
SD (%)	± 120	± 79	± 265	± 740

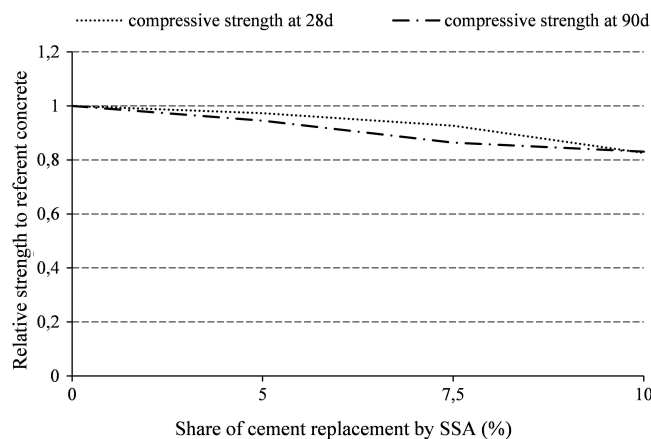


FIGURE 4 Relative compressive strength for sunflower seeds ash concrete

3 | RESULTS AND DISCUSSION

The fresh concrete properties are listed in Table 4. The results of hardened concrete properties are listed in Table 5. Figure 4 shows the compressive strength of concrete mixtures with SSA incorporated relative to the strength of reference concrete at age corresponding to 28 and 90 days. The results of the SEM analysis of the concrete specimen M0 are shown in Figure 5. Figure 6 presents the morphology of matrices that consist of hydrated cement and SSA as mineral admixtures in M5, M7.5, and M10 concretes at age of 28 days.

With respect to the fresh concrete properties listed in Table 4, the density values evidently decrease with increases in the SSA content. This result is expected because the density of SSA is lower than the density of cement (Table 1), and this, in turn, influences the density of concrete. Given the lower SSA density and higher value of fineness when compared to those of cement (Table 1), the total volume of binder increases while replacing part of the cement mass with SSA in concrete mixtures, and this further reduces the workability of concrete mixtures. Cement replacement with SSA did not significantly influence the air content in concrete.

As shown in Table 5, the compressive strength and modulus of elasticity decrease with the increases in the SSA content. For example, concrete mixtures with 10% SSA obtained 17% lower value of compressive strength at ages

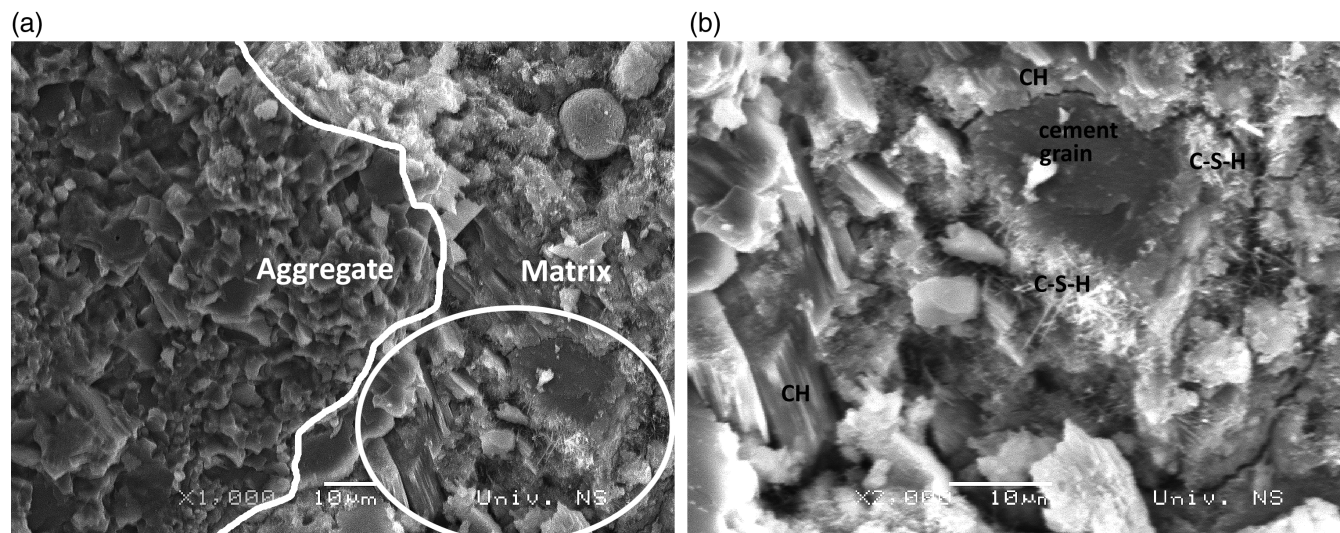


FIGURE 5 SEM images of the referent concrete, M0, after 28 days of curing (a) $\times 1,000$, (b) enlarged detail ($\times 2,000$)

corresponding to 28 and 90 days and a 12% lower value of modulus of elasticity when compared to that of the reference concrete (Figure 4). The influence of SSA on flexural strength does not appear significant, and the values of flexural strength vary between the mixtures albeit within the limits of acceptable measurement error. These facts suggest that SSA is not efficient as filler although its mean diameter (d_{50}) is 2.8 times lower than that of the cement.

The fracture surface of the M0 sample (Figure 5) is typical for a cement mortar with an inhomogeneous distribution of calcium hydroxide, C–S–H, and ettringite crystals as shown in Figure 5a (matrix). In this region, CH crystals are observed adjacent to the aggregate and C–S–H phase further in the matrix. The details in Figure 5a are enlarged and shown in Figure 5b. The presence of a loosely porous C–S–H gel is observed on the surface of the not completely reacted cement grains in the vicinity of massive column-like crystals of calcium hydroxide.

The morphologies of concrete matrices M5, M7.5, and M10 (Figure 6) were compared to the morphology of the reference matrix M0 (Figure 5). The comparison is focused on the porosity and formation of sulfate crystals. Specifically, given the existence of the physical effects of mineral admixtures known as the “dilution effect,”⁴⁷ the replacement of cement by mineral admixture results in an increase in the water/cement ratio that affects the degree of hydration of cement and the compressive strength of the material. Consequently, the porosity of the concretes with SSA increases while the strength decreases to a greater extent in the absence of the filler effect and heterogeneous nucleation. Heterogeneous nucleation is present in the early period of hydration and strongly depends on the specific surface of admixture and its surface energy. According to Ref. 47, with respect to the short-term hydration, the specific surface value of a quartz powder admixture exceeding $200 \text{ m}^2/\text{g}$ is sufficient for the occurrence of heterogeneous nucleation. The

results of the present study indicate that the obtained specific surface area value for SSA particles was $337.4 \text{ m}^2/\text{kg}$, while the particle size distribution analysis revealed that SSA contains only a low number of particles, with a mean diameter of approximately $200 \mu\text{m}$. The data indicate that the replacement of cement by SSA contributes to the phenomenon.

Comparison of the SEM image of the fractured surface of sample M0 (Figure 5) to the images in M5 (Figure 6a) and M10 (Figure 6e) indicates that the replacement of cement by SSA particles did not decrease the compactness of the matrices. Thus, it appears to lead to a more homogeneous distribution of the hydrated phase and suggests that heterogeneous nucleation occurred in the hydration process.

Conversely, the existence of large aggregates of particles (with diameters of approximately $200 \mu\text{m}$ or higher) as shown in Figures 2 and 3 could result in the absence of heterogeneous nucleation in certain parts of the sample. This is observed in Figure 6c through the presence of a significantly porous area containing clusters of SSA particles. Simultaneously, the image of the referent sample M0 in Figure 5b presents the prevailing appearance of C–S–H gel and the deposits of CH crystals while the C–S–H gel and needle-like form of the hydrated product (probably ettringite) are predominant in samples M5, M7.5, and M10, as shown in Figure 6b,d,f), respectively. This indicates the possibility that needle-like crystal forms were created through the reaction of sulfate ions from SSA and calcium hydroxide. It is highly likely that the needle-like crystal forms correspond to ettringite. The size and amount of needle-like forms increase with increase in percentage of cement replacement by SSA particles. This is potentially caused by the high concentration of SO_3 in SSA.

An alkali-silica reaction was excluded since dolomite aggregate was used in the study. The content of alkalis ($\text{Na}_2\text{O} + \text{K}_2\text{O}$) expressed as the sodium oxide equivalent for cement was 0.625, in the binder (cement + SSA) was 1.31%

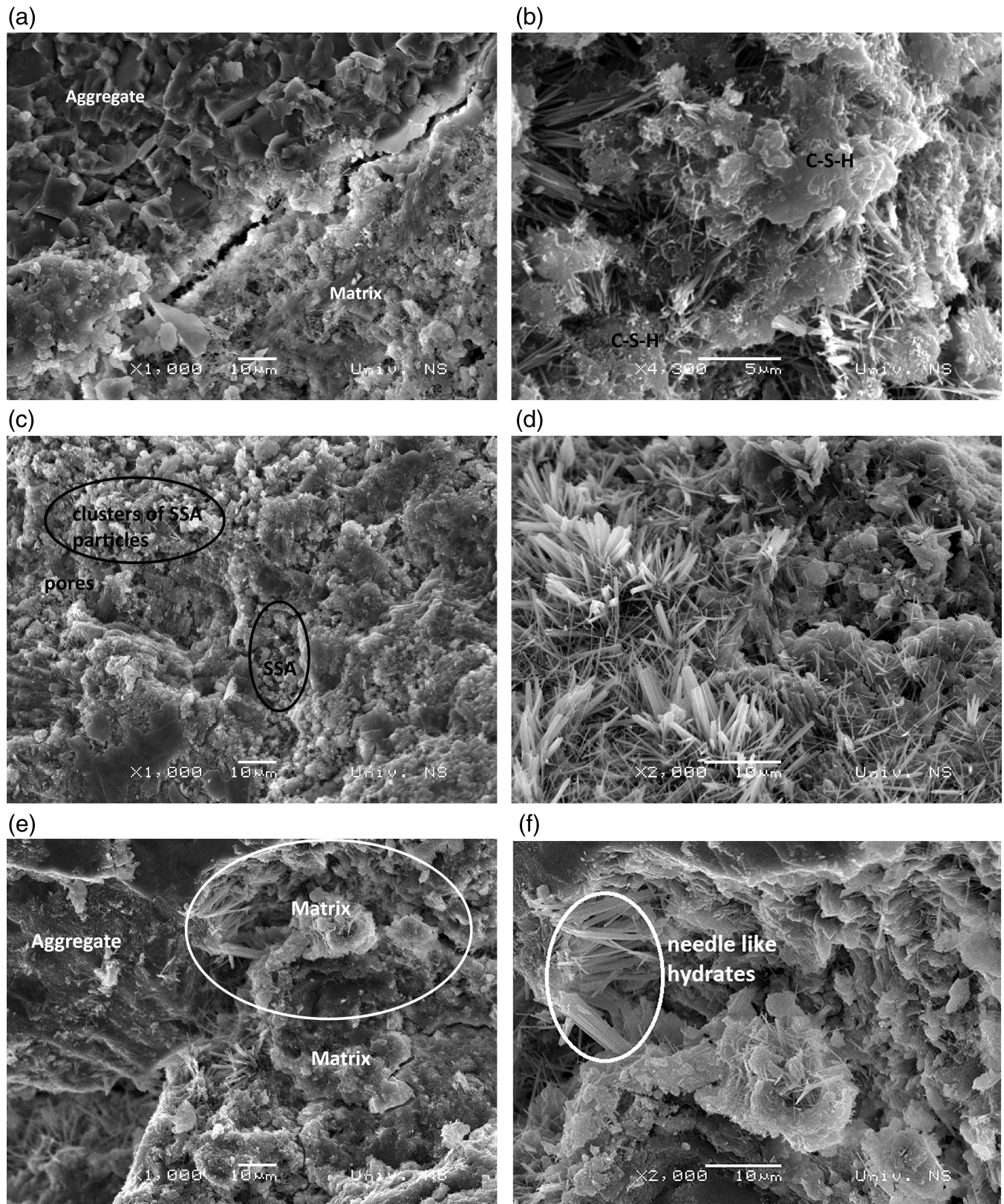


FIGURE 6 SEM images of the concretes with sunflower seeds ash as an additive after 28 days (a) concrete M5 ($\times 1,000$), (b) concrete M5 ($\times 4,300$), (c) concrete M 7.5 ($\times 1,000$), (d) concrete M 7.5 ($\times 2,000$), (e) concrete M10 ($\times 1,000$), (f) enlarged detail from the image, and (e) for concrete M10 ($\times 2,000$)

when 5% of cement was replaced by SSA, 1.656% when 7.5% was replaced, and finally approximately 2% when 10% of the cement was replaced by SSA. The SO_3 content in the binder corresponded to 0.7, 1.1, and approximately 1.45%

when 5, 7.5, and 10% of cement, respectively, was replaced by SSA. These values are in accordance with the requirements specified in standard.³³ However, the authors would like to point out that the replacement of cement mass with

SSA over 5% will adversely affect mechanical properties of concrete. Taking into account that SSA is currently available free of charge at the factory where it is generated, its use in concrete would definitely lower the final price of concrete by solving the issue of its disposal at the same time.

4 | CONCLUSION

The results presented in this study indicate that SSA does not exhibit pozzolanic activity although it does not correspond to a completely chemically inert admixture. A high content of alkalis as well as sulfate ions suggests the formation of ettringite. In addition to a certain degree of chemical effect, the mineral admixture SSA certainly influenced the appearance of the dilution effect. This effect is followed by an increase in the water/cement ratio that affects the degree of hydration of cement. The SSA median particle size ($d_{50} = 5.817 \mu\text{m}$) as well as surface area value of $337.4 \text{ m}^2/\text{kg}$ in the mineral admixture potentially influenced the filler effect and heterogeneous nucleation. The filler effect was less pronounced because the dilution effect significantly affected the strength. The presence of heterogeneous hydration is observed given the homogeneous distribution of hydration products. Based on the results, added in concrete SSA achieved all known possible effects of mineral admixtures including the filler effect, heterogenous nucleation effect, dilution effect, and a certain degree of chemical effect. The results like these could encourage the construction industry to use SSA solving thus the problem of its disposal at factories worldwide, which use shells of sunflower seeds and other types of biomass as a substitute for commonly used fuel. However, the authors would recommend the replacement of up to 5% of cement mass with SSA in concrete. Higher share of SSA as cement replacement will adversely affect mechanical properties of structural concrete. In their future research, the authors will focus on cement replacement with SSA by volume method to investigate whether it will result in higher consumption of this waste material in concrete production thus positively affecting the environment.

ACKNOWLEDGMENTS

The authors acknowledge that full financial support for this study was provided by Agricultural Waste, Challenges and Business Opportunities, Eco build project financed within Interreg IPA Cross-border Cooperation Programme Croatia-Serbia 2014–2020.

ORCID

Ivanka N. Grubeša  <https://orcid.org/0000-0002-6824-500X>

REFERENCES

1. European Parliament, Council of the European Union. Directive 2009/28/EC on the promotion of the use of energy from renewable sources. 2009 [cited xxx]. Available from: <http://eur-lex.europa.eu/legal-content/EN/ALL/?uri=celex%3A32009L0028>.

2. Loppinet-Serani A, Aymonier C, Cansell F. Current and foreseeable applications of supercritical water for energy and the environment. *ChemSusChem*. 2008;1(6):486–503.
3. Basu P. Chapter 3Biomass characteristics. Biomass gasification, pyrolysis and torrefaction: Practical design and theory. Elsevier, London, UK 2013.
4. Kattimani G, Nethravathi HM, Priyanka O, Amaravati AS, Sanjeev S. Modern soil stabilization using biomass and chemical. *Int J Innovat Res Sci Eng Tech*. 2015;4(6):4100–4103.
5. López López E, Vega-Zamanillo Á, Calzada Pérez MA, Hernández-Sanz A. Bearing capacity of bottom ash and its mixture with soils. *Soils Found*. 2015;55(3):529–535.
6. Vichan S, Rachan R. Chemical stabilization of soft Bangkok clay using the blend of calcium carbide residue and biomass ash. *Soils Found*. 2013;53(2):272–281.
7. Melotti R, Santagata E, Bassani M, Salvo M, Rizzo S. A preliminary investigation into the physical and chemical properties of biomass ashes used as aggregate fillers for bituminous mixtures. *Waste Manag*. 2013;33(9):1906–1917.
8. Cuenca J, Rodríguez J, Martín-Morales M, Sánchez-Roldán Z, Zamorano M. Effects of olive residue biomass fly ash as filler in self-compacting concrete. *Construct Build Mater*. 2013;40:702–709.
9. Aksomoglu O, Binici H, Ortlek E. Durability of concrete made by partial replacement of fine aggregate by colemanite and barite and cement by ashes of corn stalk, wheat straw and sunflower stalk ashes. *Construct Build Mater*. 2016;106:253–263.
10. Aliyu S, Yakubu KI. Wheat straw ash as cement replacement material in concrete. 2018 [cited xxx]; Available from: [www.academia.edu/23705419-WHEAT_STRAW_ASH_AS_CEMENT_REPLACEMENT_MATERIAL_IN_CONCRETE](http://www.academia.edu/23705419/WHEAT_STRAW_ASH_AS_CEMENT_REPLACEMENT_MATERIAL_IN_CONCRETE).
11. Biricik H, Aköz F, Türker F, Berktaş I. Resistance to magnesium sulfate and sodium sulfate attack of mortars containing wheat straw ash. *Cem Concr Res*. 2000;30(8):1189–1197.
12. Goyal A, Kunio H, Ogata H, et al. Synergic effect of wheat straw ash and Rice-husk ash on strength properties of mortar. *J Appl Sci*. 2007;7(21):3256–3261.
13. Matalkah F, Soroushian P, Ul Abideen S, Peyvandi A. Use of non-wood biomass combustion ash in development of alkali-activated concrete. *Construct Build Mater*. 2016;121:491–500.
14. Rajamma R, Senff L, Ribeiro MJ, et al. Biomass fly ash effect on fresh and hardened state properties of cement based materials. *Compos Part B Eng*. 2015;77:1–9.
15. Shrivastava A, Jain D. Application of different waste in concrete as a partial replacement of cement. *Int J Sci Techn Eng*. 2015;2(3):89–107.
16. Ban CC, Ken PW, Ramli M. Mechanical and durability performance of novel self-activating Geopolymer mortars. *Proc Eng*. 2017;117:564–571.
17. Rajamma R, Labrincha JA, Ferreira VM. Alkali activation of biomass fly ash–metakaolin blends. *Fuel*. 2012;98:265–271.
18. Shearer CR, Provis JL, Bernal SA, Kurtis KE. Alkali-activation potential of biomass-coal co-fired fly ash. *Cem Concr Compos*. 2016;73:62–74.
19. Demis S, Tapali JG, Papadakis VG. An investigation of the effectiveness of the utilization of biomass ashes as pozzolanic materials. *Construct Build Mater*. 2014;68:291–300.
20. Berodier E, Scrivener K. Understanding the filler effect on the nucleation and growth of C-S-H. *J Am Ceram Soc*. 2014;97(12):3764–3773.
21. Cyr M, Lawrence P, Ringot E. Efficiency of mineral admixtures in mortars: Quantification of the physical and chemical effects of fine admixtures in relation with compressive strength. *Cem Concr Res*. 2006;36:264–277.
22. De Schutter G. Effect of limestone filler as mineral addition in self-compacting concrete. 36th Conference on Our World in Concrete & Structures : 'Recent Advances in the Technology of Fresh Concrete'(OWIC'S 2011). Singapore: Ghent University, 2011; p. 49–54.
23. Lawrence P, Cyr M, Ringot E. Mineral admixtures in mortars effect of type, amount and fineness of fine constituents on compressive strength. *Cem Concr Res*. 2005;35:1092–1105.
24. Oey T, Kumar A, Bullard JW, Neithalath N, Sant G. The filler effect: The influence of filler content and surface area on Cementitious reaction rates. *J Am Ceram Soc*. 2013;96(6):1978–1990.
25. Puerta-Falla G, Kumar A, Gomez-Zamorano L, Bauchy M, Neithalath N, Sant G. The influence of filler type and surface area on the hydration rates of calcium aluminate cement. *Construct Build Mater*. 2015;96:657–665.

26. Toutanji H, Delatte N, Aggoun S, Duval R, Danson A. Effect of supplementary cementitious materials on the compressive strength and durability of short-term cured concrete. *Cem Concr Res*. 2004;34:311–319.
27. Uysal M, Yilmaz K. Effect of mineral admixtures on properties of self-compacting concrete. *Cem Concr Compos*. 2011;33:771–776.
28. Wang XY. Modeling of hydration, compressive strength, and carbonation of Portland-limestone cement (PLC) concrete. *Materials*. 2017;10(2):pii: E115.
29. Wang Y. Performance assessment of cement-based materials blended with micronized sand: Microstructure, durability and sustainability [Doctoral thesis]. Delft, the Netherlands: Faculty of Civil and Geosciences, Delft University of Technology; 2013.
30. Netinger Grubeša I, Barišić I. Environmental impact analysis of heavy metal concentrations in waste materials used in road construction. *Electron J Facul Civil Eng Osijek—e-GFOS*. 2016;13:23–29.
31. CEN (European Committee for Standardization), Brussels, Belgium. (2012). EN 933–1 tests for geometrical properties of aggregates—Part 1: Determination of particle size distribution—sieving method.
32. CEN (European Committee for Standardization), Brussels, Belgium. (2013). EN 1097–6, tests for mechanical and physical properties of aggregates—Part 6: Determination of particle density and water absorption.
33. CEN (European Committee for Standardization), Brussels, Belgium. (2011). EN 197–1, cement—Part 1: Composition, specifications and conformity criteria for common cements.
34. CEN (European Committee for Standardization), Brussels, Belgium. (2013). EN 196–2, method of testing cement—Part 2: Chemical analysis of cement.
35. CEN (European Committee for Standardization), Brussels, Belgium. (2010). EN 196–6, methods of testing cement—Part 6: Determination of fineness.
36. CEN (European Committee for Standardization), Brussels, Belgium. (2012). EN 450–1, Fly ash for concrete—Part 1: Definition, specifications and conformity criteria.
37. Mo L, Deng M, Tang M, Al-Tabbaa A. MgO expansive cement and concrete in China: Past, present and future. *Cem Concr Res*. 2014;57:1–12.
38. Nokken MR. Expansion of MgO in cement pastes measured by different methods. *ACI Mater J*. 2010;107(1):80–84.
39. ISO (International Organization for Standardization). (2009). ISO 13320, Particle size analysis—laser diffraction methods.
40. CEN (European Committee for Standardization), Brussels, Belgium. (2009). EN 12350–2, Testing fresh concrete—Part 2: Slump-test.
41. CEN (European Committee for Standardization), Brussels, Belgium. (2009). EN 12350–6, testing fresh concrete—Part 6: Density.
42. CEN (European Committee for Standardization), Brussels, Belgium. (2009). EN 12350–7, Testing fresh concrete—Part 7: Air content. Pressure methods.
43. CEN (European Committee for Standardization), Brussels, Belgium. (2009). EN 12390–2, testing hardened concrete—Part 2: Making and curing specimens for strength tests.
44. CEN (European Committee for Standardization), Brussels, Belgium. (2009). EN 12390–3, Testing hardened concrete—Part 3: Compressive strength of test.
45. CEN (European Committee for Standardization), Brussels, Belgium. (2009). EN 12390–5, Testing hardened concrete—Part 5: Flexural strength of test specimens.
46. CEN (European Committee for Standardization), Brussels, Belgium. (2013). EN 12390–13, testing hardened concrete—Part 13: Determination of secant modulus of elasticity in compression.
47. Lawrence P, Cyr M, Ringot E. Mineral admixtures in mortars: Effect of inert materials on short-term hydration. *Cem Concr Res*. 2003;33:1939–1947.

AUTHORS DETAILS



Ivanka N. Grubeša, Associate Professor
Faculty of Civil Engineering Osijek
Josip J. Strossmayer University of Osijek
Drinska 16a, 31000 Osijek, Croatia
nivanka@gfos.hr



Miroslava Radeka, Professor
Department of Civil Engineering and Geodesy
Faculty of Technical Sciences
University in Novi Sad
Trg Dositeja Obradovića 6, 21000
Novi Sad, Serbia
mirka@uns.ac.rs



Mirjana Malešev, Professor
Department of Civil Engineering and Geodesy
Faculty of Technical Sciences
University in Novi Sad
Trg Dositeja Obradovića 6, 21000
Novi Sad, Serbia
miram@uns.ac.rs



Vlastimir Radonjanin, Professor
Department of Civil Engineering and Geodesy
Faculty of Technical Sciences
University in Novi Sad
Trg Dositeja Obradovića 6, 21000
Novi Sad, Serbia
radonv@uns.ac.rs



Anita Gojević, Civil Engineer
Josip Juraj Strossmayer University of Osijek
Trg Sv. Trojstva 3, 31000 Osijek,
Croatia
anitagojevic@gmail.com



Rafat Siddique, Professor
Department of Civil Engineering
Thapar University
Patiala 147004, Punjab, India
rsiddique@thapar.edu

How to cite this article: Grubeša IN, Radeka M, Malešev M, Radonjanin V, Gojević A, Siddique R. Strength and microstructural analysis of concrete incorporating ash from sunflower seed shells combustion. *Structural Concrete*. 2019;20:396–404. <https://doi.org/10.1002/suco.201800036>